LEACHING KINETICS OF COPPER FROM CHALCOPYRITE CONCENTRATE IN NITROUS-SULFURIC ACID

Ozge GOK[*], Corby G. ANDERSON[**], Gorkem CICEKLI[*], E. Ilknur COCEN[*]

[*]   Mining Engineering Dept., Faculty of Engineering, Dokuz Eylul University, Izmir, 35160, Turkey;
      e-mail: ozge.solak@deu.edu.tr)
[**] Department of Metallurgical and Materials Engineering, Colorado School of Mines, CO, 80401, USA

Abstract: Treating chalcopyrite flotation concentrates by hydrometallurgical techniques seems to be the most convenient method for leaching copper due to concerns over air pollution and regulations regarding the emission of sulfur dioxide that result from smelting. In this study, the leaching recovery-time trajectories of bulk chalcopyrite concentrate obtained from a flotation plant in the Kastamonu region of Turkey are presented. The effects of various parameters were elucidated in the nitrous-sulfuric acid electrolyte (C_{NaNO2}:0.05 M–0.15 M, C_{H2SO4}:1 M) at a moderate temperature (80–120 °C). A high level of copper recovery (98%) from bulk chalcopyrite concentrate was obtained under a total pressure of 6 atm at 120°C within 2 h when using small amounts of nitrite species due to their autocatalytic behavior in acidic solutions. The kinetics were well correlated with the shrinking core model for the diffusion controlled mechanism with an apparent activation energy of 34.06 kJ·mol^{-1}. Elemental sulfur was the primary leaching product on the mineral surface, as confirmed using XRD and SEM/EDX. The semi-empirical equation explaining the reaction rate under the present conditions was expressed as follows:

$$1-\frac{2}{3}X-(1-X)^{\frac{2}{3}}=56.53\cdot10^{-4}C_{NaNO_2}^{0.96}\gamma_0^{-0,83}e^{-\frac{4096.7}{T}t}.$$

Keywords: chalcopyrite, pressure leaching, nitrogen species, kinetics

Introduction

Concerns over air pollution and strict environmental regulations regarding the emission of sulfur dioxide, combined with the increased demand of treating complex chalcopyrite ores and concentrates with high recoveries, have led to the development of hydrometallurgical processes as alternatives to smelting. Advances in construction materials, successful implementation of autoclave technology and development of
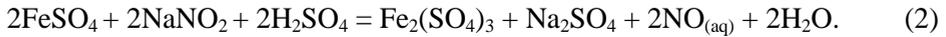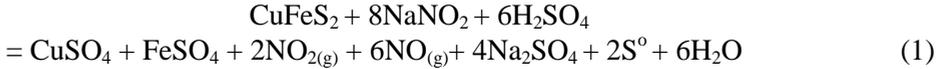
more efficient mills for the fine or ultrafine grinding of sulfides have made chalcopyrite concentrate leaching more reliable and cost-competitive (Wang, 2005).

In the last two decades, although some hydrometallurgical processes have been conducted at the lab/pilot scale, only a few have been built at the plant scale (Corrans and Angove, 1993; Dreisinger et al., 2003; Jones, 1996; Kofluk and Collins, 1998; Dreisinger et al., 2002; Stanley and Submanian, 1977; Ferron et., 2001; Marsden et al., 2003). Typically, most of these methods promote the oxidation of copper from chalcopyrite concentrate in the presence of several species such as ferric ions, ferrous ions, cupric ions, silver ions, bacteria, pyrite and oxygen (Dixon et al., 2008; Dreisinger and Abed, 2002; Dutrizac et al., 1969; Hackl et al., 1995; Hirato et al., 1987; Hiroyoshi et al., 2000; Linge, 1976; Miller and Portillo, 1979; Munoz et al., 1979).
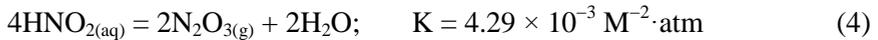
Sulfuric acid processing with the addition of a small amount of nitrogen species has been employed for a long time in some industrial applications. The first patented commercial process by Sunshine Precious Metals (Idaho, USA) used a sulfuric and dilute nitric acid mixture to leach silver- and copper-bearing ores (Caldon, 1978). Subsequently, "nitric acid" leaching was practiced under various process acronyms such as NSL (Brennecke et al., 1981), NITROX (Van Weert et al., 1986), ARSENO, and REDOX (Beattie et al., 1989). More recently, a novel process involving nitrogen species-catalyzed pressure leaching (NSC) was commissioned and performed successfully on an industrial scale at Sunshine Precious Metals (Anderson et al., 1992; Anderson et al., 1993). It was reported that silver and copper were successfully recovered from a complex sulfide concentrate at temperatures between 145°C and 155°C and at a total pressure of 7 atm (Ackerman et al., 1993). The NSC pretreatment process was proposed as a potential alternative process capable of being performed at "modest" process temperatures and pressures (125-170°C and 6-10 atm) and with a lower oxygen demand (associated with the partial oxidation of sulfide to zero-valence sulfur). The process employs sulfuric acid to achieve high proton activity, oxygen/air as the primary oxidant, and a low concentration of nitrite, which, in a broad sense, acts in a "catalytic" role (Baldwin and Van Weert, 1996; Anderson, 2003). The reasons for favoring nitrogen species are (i) they are powerful oxidizing agents, (ii) the NO_x gases produced (NO, NO_2, etc.) remove other reaction products from the mineral surfaces, (iii) high temperatures increase the reaction rates, and (iv) the oxidant can be regenerated autocatalytically.

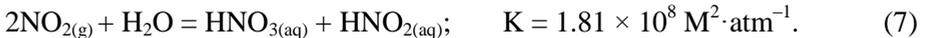## Reaction Sequence of Chalcopyrite Dissolution

The complex chemistry of chalcopyrite leaching in acidic nitrite electrolyte can be explained based on data (Gok and Anderson, 2013) for the $CuFeS_2$-H_2SO_4-$NaNO_2$-H_2O system as follows:

$$CuFeS_2 + 8NaNO_2 + 6H_2SO_4$$
$$= CuSO_4 + FeSO_4 + 2NO_{2(g)} + 6NO_{(g)} + 4Na_2SO_4 + 2S^o + 6H_2O \tag{1}$$

$$2FeSO_4 + 2NaNO_2 + 2H_2SO_4 = Fe_2(SO_4)_3 + Na_2SO_4 + 2NO_{(aq)} + 2H_2O. \tag{2}$$

In that study, it was found that both nitric oxide ($NO_{(g)}$) and nitrogen dioxide ($NO_{2(g)}$) were most likely to be generated as products of chalcopyrite leaching with nitrite. During the oxidation, in addition to $NO_{(g)}$ and $NO_{2(g)}$, the system may contain a number of other nitrogen compounds (HNO_2, N_2O_4, NO_2^-, N_2O_3, HNO_3 and NO_3^-) that have various catalytic activities. Nitrous acid (HNO_2) has been predicted to be the most kinetically reactive form when nitrite salt is introduced into the acidic solution. The two-step disproportionation reaction mechanism of HNO_2 to $NO_{(g)}$ and $NO_{2(g)}$ has been described by Eqs. 3-5 (Park and Lee, 1988).

$$NaNO_{2(aq)} + H^+ = HNO_{2(aq)} + Na^+ \qquad K = 2.51 \times 10^3 \tag{3}$$

$$4HNO_{2(aq)} = 2N_2O_{3(g)} + 2H_2O; \qquad K = 4.29 \times 10^{-3} \text{ M}^{-2} \cdot \text{atm} \tag{4}$$

$$2N_2O_{3(g)} = 2NO_{(g)} + 2NO_{2(g)}; \qquad K = 1.91 \text{ atm.} \tag{5}$$

The convincing work by Markovitz et al. (1981) showed that the rate of homolysis of $N_2O_{3(g)}$ to $NO_{(g)}$ and $NO_{2(g)}$ was much greater than hydrolysis to HNO_2. Nitric oxide is more likely to be in the gas phase due to its lower solubility and is re-oxidized to HNO_2 in the oxidizing environment (Awad and Stanbury, 1993), as indicated in Eq. 6. Nitrogen dioxide immediately reacts with water to form two oxyacids, nitric acid and nitrous acid (Kameoka and Pigford, 1977), according to Eq. 7. The cyclic NO_x redistribution mechanism is completed by this equilibrium, and only one fourth of the initial amount of nitrous acid is lost. Finally, all of the nitrogen species that evolve in the electrolyte from the nitrite salt, except $NO_{(g)}$, are oxidized to nitrate (NO_3^-) (Gok, 2009).

$$2NO_{(aq)} + \tfrac{1}{2} O_{2(aq)} + H_2O \rightarrow 2HNO_{2(aq)} \tag{6}$$

$$2NO_{2(g)} + H_2O = HNO_{3(aq)} + HNO_{2(aq)}; \qquad K = 1.81 \times 10^8 \text{ M}^2 \cdot \text{atm}^{-1}. \tag{7}$$

The reaction scheme explained above takes into account both the steady-state absorption of NO_x gases into the electrolyte and the disproportionation reactions. These non-elementary reaction steps also give a more complete understanding of the regeneration process.

The present study provides an extensive investigation into the leaching kinetics of copper from bulk chalcopyrite concentrate in nitrous-sulfuric acid with an emphasis on the roles of temperature, initial nitrite concentration, and particle size, which have not been sufficiently studied from a theoretical or practical point of view.

Material and Methods

Materials

Experiments were implemented with bulk concentrate obtained from the Küre Copper Concentrator Plant, Eti Bakır A.Ş., Kastamonu-Turkey, where $CuFeS_2$–ZnS-FeS_2 complex ore is treated. The chemical and mineralogical compositions of the ''as-received'' bulk concentrate are presented in Table 1.

Mineralogical analyses performed by scanning electron microscopy (SEM) coupled with energy dispersive spectroscopy (EDS) and X-ray diffraction of the bulk concentrate revealed that the sample contained mainly chalcopyrite with sphalerite, pyrite and small amounts of bornite. The primary gangue mineral was quartz. Chemical analyses by atomic absorption spectrometry (AAS) in conjunction with the mineralogical findings were used to determine mineralogical composition.

Table 1. Results of the chalcopyrite concentrate head sample assay

Chemical Analysis		Mineralogical Analysis	
Element	%	Mineral	%
Cu	11.21	$CuFeS_2$	28
Fe	32.36	Cu_5FeS_4	3
Zn	5.10	ZnS	8
S	36.8	FeS_2	51
Co	0.06	SiO_2	4
Pb	0.02	CaO	0.35
Ag (g/t)	27		

Experimental Procedure

Experiments were conducted using a Parr 1 L 4520 M model vertical reactor constructed from titanium and controlled to within ±2 °C using a Parr 4843 model temperature controller. Typically, the vessel was charged with electrolyte containing $NaNO_2$, H_2SO_4 and 5% w/v pulp density bulk chalcopyrite concentrate. Sodium nitrite immediately dissociated to produce nitrous acid in acid solution as described in Eq. 3. The experiments were initiated by introducing nitrite salt into the electrolyte at a concentration of 0.05–0.15 M. The system was then pressurized with oxygen on a continuous basis to maintain a total pressure of 6 atm. The temperature of the solution was varied over the range of 80–120 °C and the reaction sustained for 2 h. The initial sulfuric acid concentration was 1.0 M and the reaction was mixed well by stirring at 400 rpm by a magnetically driven twin impeller. Samples from each experiment were taken at the selected time intervals and analyzed using an atomic absorption spectrophotometer (Analytik Jena NovaA 300). XRD and SEM analyses were performed using a Rigaku Miniflex II diffractometer with Cu Kα radiation and a JEOL JXA-733 Superprobe, respectively. The particle size (d_{80}) of the received

samples, determined from measurements on an HORIBA/Partica LA-950V2 Particle Size Analyzer, was 35 μm. Ultrafine milling of the as-received material to 15 μm was performed using a ball mill. The size of the product was confirmed by particle size analysis.

Results and Discussion

Effects of parameters

The influence of the concentration of nitrite on copper recovery was investigated using an electrolyte containing various initial sodium nitrite concentrations in the range of 0.05 M–0.15 M at 120 °C. The results are plotted in Fig. 1. Although the recovery-time curves overlapped during the first 15 min, the reaction rates were enhanced after the dissociation of nitrite into $NO_{2(g)}$ and $NO_{(g)}$ in acidic electrolyte. Additionally, the *in situ* regeneration of NO_x during the dissolution process minimized the need to add additional exogenous nitrite over the course of the reaction.

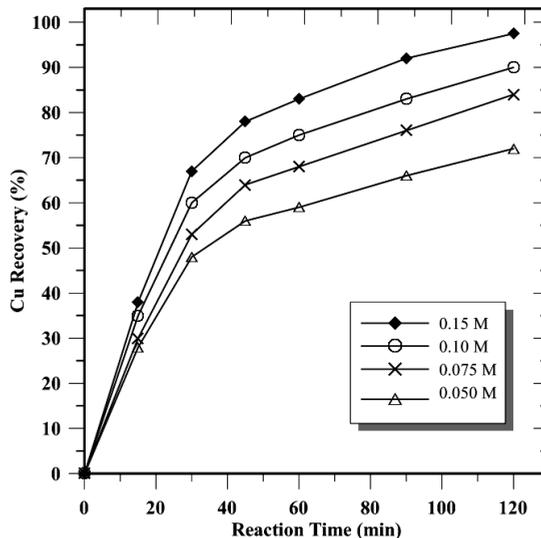Fig. 1. Effect of the nitrite concentration on copper recovery. Initial electrolyte conditions: $C_{H_2SO_4}$ =1 M, d_{mean} = 15 μm, T = 120°C, P_{tot} = 6 atm

The extraction of copper at various temperatures (80–120 °C) was implemented in the electrolyte containing 0.10 M $NaNO_2$ and 1 M H_2SO_4 as depicted in Fig. 2. Copper recovery was enhanced by increasing temperature; 90% extraction was obtained at 120 °C, whereas only 60% copper extraction was obtained at 80 °C within 2 h. This is likely due to slower dissolution kinetics as temperature decreases due to the increasing viscosity of molten sulfur (Papangelakis, 2005).
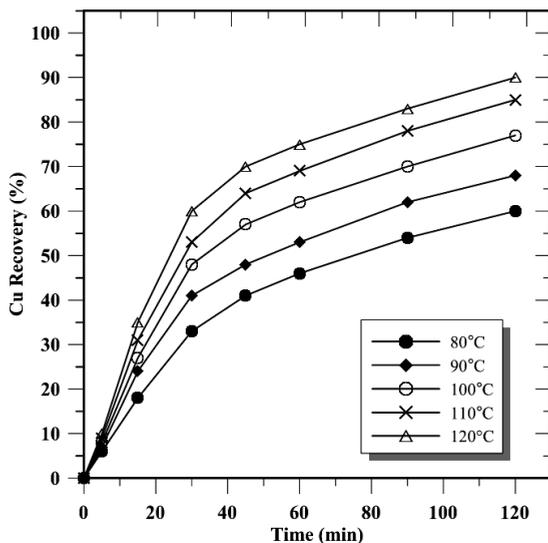
Fig. 2. Effect of the temperature on copper recovery. Initial electrolyte conditions:
$C_{NaNO_2} = 0.10$ M, $C_{H_2SO_4} = 1$ M, $d_{mean} = 15$ μm, $P_{tot} = 6$ atm

In this study, a set of grinding tests were performed to determine the effect of particle size on copper recovery. Tests were performed for three different particle sizes (35 μm, 25 μm, and 15 μm) at 120 °C under a total pressure of 6 atm. The results are illustrated in Fig. 3. Reducing the material size significantly increased copper recovery

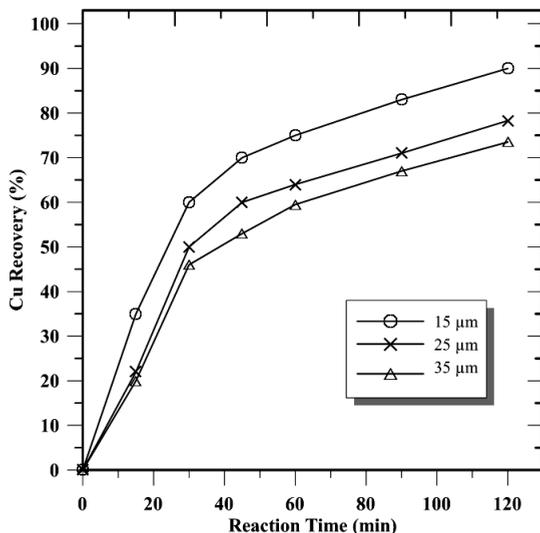Fig. 3. Effect of the particle size of concentrate on copper recovery. Initial electrolyte conditions:
$C_{NaNO_2} = 0.10$ M, $C_{H_2SO_4} = 1$ M, T = 120°C, $P_{tot} = 6$ atm

(from 70% to 90%). These findings revealed that this is a classic heterogeneous reaction system in which the larger surface area due to the smaller particle size has a beneficial effect. Similar behavior has been reported for the nitric-sulfuric acid system (Anderson et al., 1991). Researchers have explained that this type of dramatic improvement in conversion is usually indicative of a reaction controlled by diffusional effects. Less encapsulation of the particle in molten sulfur could be observed by grinding the material to increase its total surface area. Size reduction also enables more copper to be solubilized by generating more NO and NO_2 gas according to the reaction shown in Eq. 1.

Kinetic Analysis

A non-catalytic heterogeneous reaction model was conducted to evaluate the kinetic parameters and the rate-controlling step of the chalcopyrite dissolution in acidic nitrite solutions. The rate controlling step of the reaction between solid particles and electrolyte can be due to one of the following: external diffusion of the reactant through the boundary layer of the fluid surrounding the particle, reaction on the surface between the fluid reactant and the solid, or internal diffusion of the reactant through the reaction products on the particle (Levenspiel, 1972; Mazet, 1992). Three shrinking core models were tested to better understand the leaching mechanism of chalcopyrite in acidic nitrite solutions (Aydogan et al., 2005; Levenspiel, 1972):

$$X = \frac{3b'k_gC_A}{\rho_B r_o}t \qquad \text{(film diffusion control)} \qquad (8)$$

$$1-(1-X)^{\frac{1}{3}} = \frac{b'k_rC_A}{\rho_B r_o}t \qquad \text{(surface chemical reaction control)} \qquad (9)$$

$$1-\frac{2}{3}X-(1-X)^{\frac{2}{3}} = \frac{2b'k_d D_e C_A}{\rho_B r_o^{\,2}}t \qquad \text{(ash diffusion control).} \qquad (10)$$

Rate constant values and their correlation coefficients in these models are presented in Table 2. Detailed analysis of the data revealed that diffusion through the product layer is the limiting step in the dissolution reaction. Therefore, subsequent linearization of the values obtained from temperature-, particle size- and nitrite concentration-related experiments was performed by the model equation $1 - 2/3X - (1 - X)^{2/3} = k_d t$. The model plots for nitrous acid concentration and temperature are given in Fig. 4 and Fig. 5. Apparent rate constants k_1 and k_2 were found from the slopes of the straight lines.

O. Gok, C.G. Anderson, G. Cicekli, E.I. Cocen

Table 2. Apparent rate constants and correlation coefficients for shrinking core model

|	Surface chemical reaction $1 - (1 - X)^{1/3}$		Diffusion through product layer $1 - 2/3X - (1 - X)^{2/3}$	
	k_r (min^{-1})	R^2	k_d (min^{-1})	R^2
Concentration (M)				
0.05	0.0035	0.7019	0.008	0.9768
0.075	0.0044	0.8199	0.012	0.9840
0.10	0.0052	0.8238	0.016	0.9830
0.15	0.0066	0.9008	0.023	0.9902
Particle Size (mm)				
0.035	0.0035	0.8203	0.0008	0.9812
0.025	0.0039	0.8014	0.0010	0.9798
0.015	0.0052	0.8238	0.0016	0.9830
Temperature (K)				
353	0.0026	0.8411	0.0005	0.9939
363	0.0031	0.8031	0.0007	0.9928
373	0.0038	0.8032	0.0010	0.9860
383	0.0045	0.8377	0.0013	0.9890
393	0.0052	0.8238	0.0016	0.9830
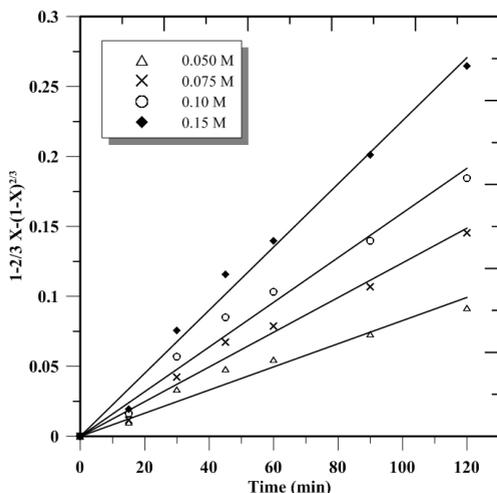
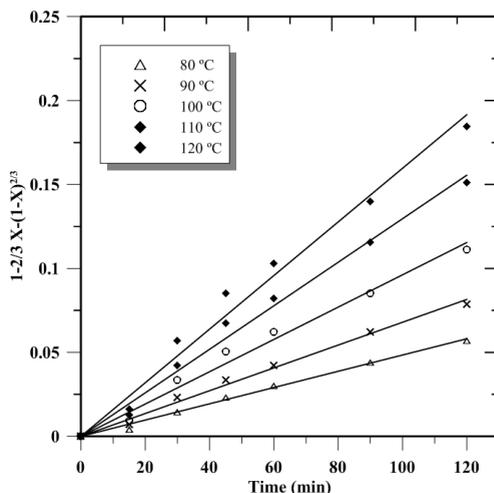Fig. 4. Plot of the shrinking core model for the effect of nitrite concentration on the reaction rate

Fig. 5. Plot of the shrinking core model for the the effect of temperature on the reaction rate

When temperature is selected as a variable factor, activation energy of the leaching reaction can be calculated by the expression below. The value of activation energy, E_a, and the pre-exponential factor, A, are estimated to be 34.06 kJ·mol^{-1} and 56.26 min^{-1}, respectively, from Fig. 6.

$$k_d = A e^{\frac{-E_a}{RT}} \qquad (11)$$

Typically, low activation energy (<20 kJ·mol^{-1}) confirms the presence of a diffusion-controlled system (Jackson, 1982). However, Baba et al. (2009) and Olanipekun (1999) have claimed that some diffusion-controlled reactions have unexpectedly high activation energies (Tsuchida et al., 1982; Baba and Adekola, 2010).
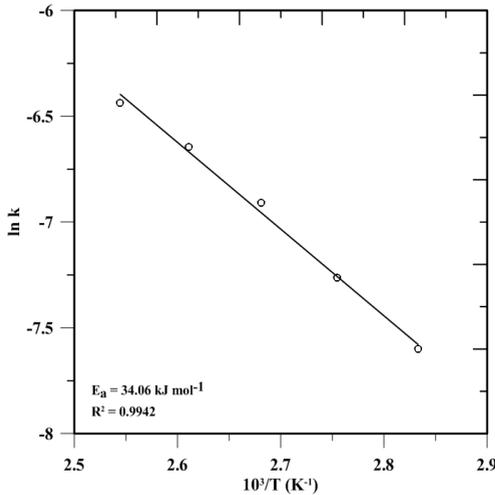

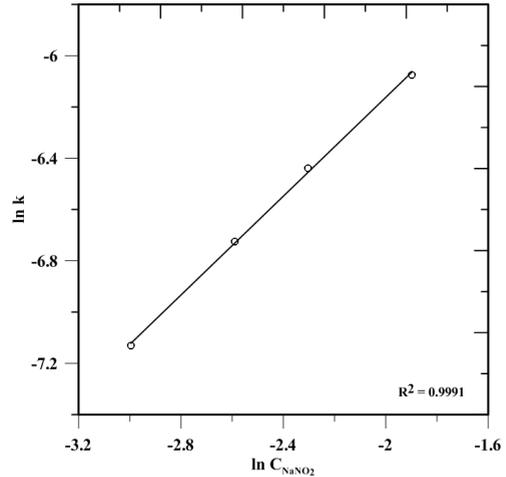Fig. 6. Plot of parabolic leaching rate constants vs. inverse of temperature (Arrhenius plot)

Fig. 7. Determination of reaction order for chalcopyrite dissolution in acidic nitrite electrolyte

It should be noted that in some instances the rate controlling mechanism of the heterogeneous dissolution process can be predicted better from the kinetic equations rather than the activation energy. Aydogan et al. (2007) demonstrated that a diffusion-controlled process is slightly dependent on temperature, while the chemically controlled process is strongly dependent on temperature. Researchers found the activation energy to be 42.26 kJ·mol^{-1} in the range of 27–60 °C for the Turkish galena concentrate in 0.5 M HNO$_3$ and 1.0 M H$_2$O$_2$ electrolyte. Based on discussions in literature and the correlation coefficients given in Table 2, it was concluded that the dissolution mechanism is controlled by diffusion through the product layer.

The effect of nitrite concentration on the reaction rate was investigated from a plot of $\ln k_1$ vs. $\ln C_{HNO2}$. The slope of the plot (Fig. 7) reveals that the reaction order is 0.96 with respect to nitrous acid. Aydogan et al. (2007) obtained a similar reaction order for leaching in nitric acid and hydrogen peroxide.

To elucidate the rate-determining step for this study, kinetic curves (presented in Fig. 3) were linearized by means of Eq. 10. Generally, if diffusion controls the reaction rate, there is a linear relation between the apparent rate constant, k_3, and the

reciprocal of the square of particle radius, $1/r_0^2$. A linear dependence between k and $1/r_0^2$ values is observed in Fig. 8 which confirms that diffusion through the product layer is the rate-limiting step for this process.

A semi-empirical model describing the effects of the reaction parameters on the rate constant of the reaction can be written as follows:

$$k_d = k_o C^a \gamma_o{}^b e^{\frac{-E_a}{RT}} . \tag{12}$$

Combining Eqs. (11) and (12), the following equation is obtained:

$$1 - \frac{2}{3}X - (1-X)^{\frac{2}{3}} = k_o C^a \gamma_o{}^b e^{\frac{-E_a}{RT}} t \tag{13}$$
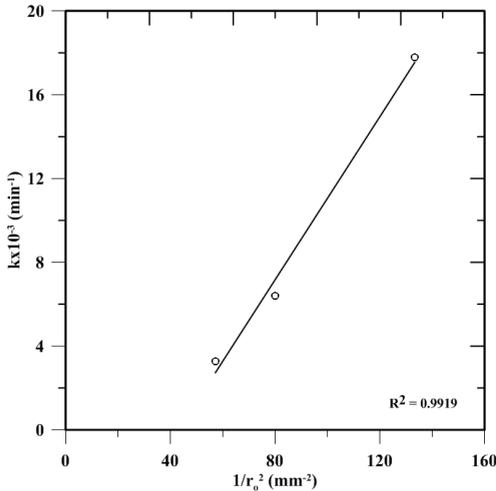

Fig. 8. Dependence of rate constant
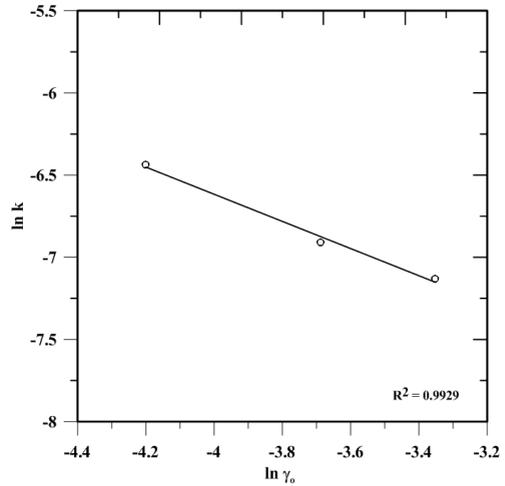on particle size radius

Fig. 9. Determination of constant b
in semi-empirical model equation

The constant a was estimated to be 0.96 from the slope of the line in Fig. 7. The order of the initial particle radius, b, was found to be –0.83 from the $\ln k$ vs. $\ln \gamma_o$ plot in Fig. 9. Substituting the values of a, b, and E_a into Eq. 13, the value of k_o is calculated to be $56.53 \cdot 10^{-4}$. Hence, the proposed model equation to describe chalcopyrite leaching in acidic nitrite electrolyte is described as follows:

$$1 - \frac{2}{3}X - (1-X)^{\frac{2}{3}} = 56.53 \cdot 10^{-4} C_{NaNO_2}^{0.96} \gamma_o{}^{-0.83} e^{\frac{-4096.7}{T}} t . \tag{14}$$

The agreement between experimental results and theoretical calculations (Eq. 13) was tested (Fig. 10). The correlation is reasonably satisfactory and suggests that Eq. 14 can be used to predict the leaching rate for the ranges of particle size, acid concentrations and temperatures used in this study.
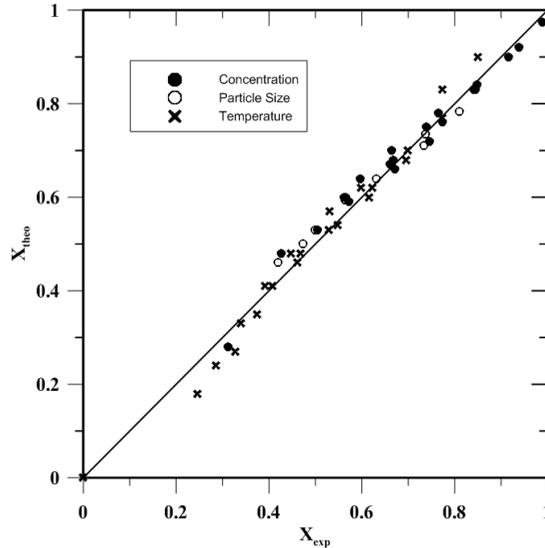

Fig. 10. Correlation of the observed and estimated values of reaction rate constants

Characterization of Solid Residue

Chemical (AAS) and physical analyses (SEM and XRD) were performed to explain the behavior of the sulfide concentrate during the leaching of chalcopyrite with nitrite. Chemical analyses of the solid residue indicated that during the first hour most of the pyrite and sphalerite were leached. The dissolution of chalcopyrite, pyrite and sphalerite over time can also be observed from the XRD analyses of the head sample (Fig. 11a) and residues obtained after 2 h (Fig. 11b). SEM micrographs and X-ray diffraction spectra revealed non-conductive sulfur layers and quartz to be the major components. The micrographs and spectra of product layers formed on the particle surface are presented in Fig. 11 and Fig. 12 for the optimum chalcopyrite dissolution conditions: 0.10 M $NaNO_2$, 1 M H_2SO_4 at 393 K. As the sulfur layer builds, it impedes the reaction so that diffusion through the product layer is a major reaction barrier. However, it is clear that the formation of elemental sulfur does not hinder the reaction within two hours at higher temperatures.
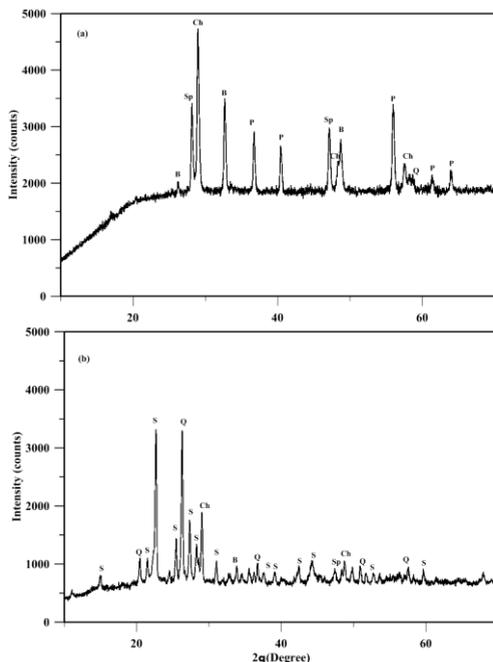
Fig. 11. XRD patterns of (a) bulk concentrate, (b)
solid residue at 120 °C after 2 h. In the figure:
Ch = chalcopyrite, P = pyrite, Sp = sphalerite,
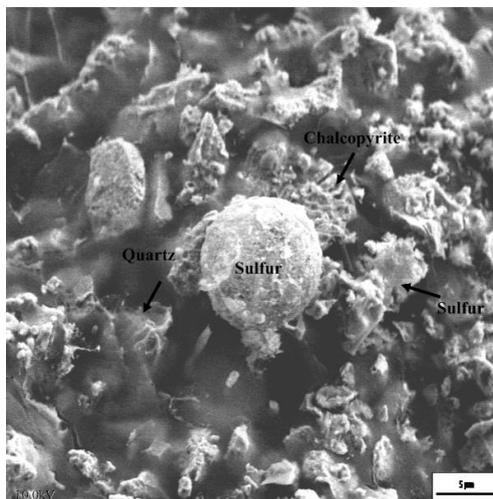B = Bornite, S = Sulfur, Q = Quartz

Fig. 12. SEM micrographs of solid residue at 120 °C
after 2 h at magnification 1500×

Conclusions

The kinetics of dissolution of bulk chalcopyrite concentrate in acidic nitrite electrolyte have been investigated in the temperature range of 80–120 °C. On the basis of the results provided by the experiments, the following can be concluded.

- An increase in nitrite concentration from 0.05 M to 0.15 M caused a significant increase in leaching from 72% to 98% over the course of 120 min.
- The dissociation products of nitrous acid, NO and NO_2, were realized during the withdrawn of the liquid samples. The rapid extraction of copper from the complex mineral matrix with such small amounts of nitrite revealed that NO reacted with oxygen to regenerate HNO_2. Accordingly, nitrous acid could follow a second reaction path by reacting with a nitrate ion, reducing the nitrate to form NO_2 and water. The key intermediate product of the reaction, nitrous acid, serves both to reduce nitrate and to oxidize NO. Overall, more nitrous acid is produced than consumed.

- The leaching of chalcopyrite concentrate with a particle size of 15 μm in nitrite-containing solutions had a high reaction rate. Over 98% of the copper was dissolved in 120 min at 120 °C. Pyrite and sphalerite were completely dissolved within 120 min, as confirmed with X-ray diffraction measurements.
- The extraction of copper obeyed a shrinking core model with a diffusion-controlled mechanism in which the diffusion through the product layer was the rate-limiting step. The value of activation energy was calculated to be 34.06 kJ·mol^{-1} and the reaction order with respect to nitrite concentration was 0.96. This is consistent with the following semi-empirical relation:

$$1 - \frac{2}{3} X - (1-X)^{\frac{2}{3}} = 56.53 x 10^{-4} C_{\text{NaNO}_2}^{0.96} \gamma_o^{-0.83} e^{\frac{-4096.7}{T}} t \, .$$

- The results of the post-leaching process indicated the presence of a residue containing elemental sulfur and quartz as its major constituents. This was confirmed by both X-ray diffraction spectra and SEM micrographs.

Acknowledgement

References

ACKERMAN J.B., ANDERSON C.G., NORDWICK S.M., KRYS L.E., 1993. *Hydrometallurgy at the Sunshine Mine metallurgical complex*. In: Hiskey B., Wadsworth M. (Eds.), Proceedings of AIME Meeting, Hydrometallurgy-Fundamentals, Technology and Innovations, Littleton, Colorado, 477–498.

ANDERSON C.G., KRYS, L.E., HARRISON, K.D., 1992. *Treatment of metal bearing mineral material*. Chemical Abstract, US Patent No. 5096486.

ANDERSON C.G., HARRISON K.D., KRYS L.E., 1993. *Process Integration of sodium nitrite oxidation and fine grinding in refractory precious metal concentrate pressure leaching*. In: Mishra R.K. (Ed.), *Precious Metals*, Allentown, Pennsylvania, 19-45.

ANDERSON C.G., HARRISON K.D., KRYS L.E., 1996. *Theoretical considerations of sodium nitrite oxidation and fine grinding in refractory precious metals concentrate pressure leaching*. Minerals and Metallurgical Processing, AIME-SME, 4.

ANDERSON C.G., 2003, *Treatment of copper ores and concentrates with industrial nitrogen species catalyzed pressure leaching and non-cyanide precious metals recovery*. J. Metals, 55, 32–36.

AYDOGAN S., ARAS A., CAMBAZOGLU M., 2005, *Dissolution kinetics of sphalerite in acidic ferric chloride leaching*. Chem. Eng. J., 114, 67–72.

AYDOGAN S., ARAS A., UCAR G., ERDEMOGLU M., 2007, *Dissolution kinetics of galena in acetic acid solutions with hydrogen peroxide*. Hydrometallurgy, 89, 189–195.

AWAD H.H., STANBURY D.M., 1993, *Autooxidation of NO in aqueous solution*, Int. J. Chem. Kin., 25, 375–381.

BABA A.A., ADEKOLA F.A., BALE, R.B., 2009, *Study of dissolution kinetics of a Nigerian cassiterite ore by hydrochloric acid*. Sci. Focus, 14 (2), 198–207.

BABA A.A., ADEKOLA F.A., 2010, *Hydrometallurgical processing of a Nigerian sphalerite in hydrochloric acid: characterization and dissolution kinetics*. Hydrometallurgy, 101 (1–2), 69–75.

BALDWIN S.A., VAN WEERT G.V., 1996, *On the catalysis of ferrous sulphate oxidation in autoclaves by nitrates and nitrites*. Hydrometallurgy, 42, 209–219.

BEATTIE M.J.V., RANDSEPP R., ISMAY A., 1989. *Arseno/Redox Process for Refractory Gold Ores*. in: Dobby, G.S., Rao, S.R. (Eds.), Intern. Symp. Processing Complex Ores, Pergamon, Oxford, 431–439.

BRENNECKE H.M., BERGMANN O., ELLEFSON R.R., DAVIES D.S., LEUDERS R.E., SPITZ R.A., 1981, *Nitric-sulfuric leach process for recovery of copper from concentrate.* J. Min. Eng., 12, 20–24.

CALDON F., 1978. *Treatment of metal bearing mineral material*. Chemical Abstract, US Patent No. 4084961.

CORRANS I.J., ANGOVE J.E., 1993. *Activation of a Mineral Species*, Chemical Abstract, US Patent No 232491.

DIXON D.G., MAYNE D.D., BAXTER K.G., 2008, *Galvanox^{TM} – a novel galvanically assisted atmospheric leaching technology for copper concentrate*. Canadian Metallurgical Quarterly, 47, 327–336.

DREISINGER D., ABED N.A., 2002, *Fundamental study of the reductive leaching of chalcopyrite using metallic iron part I: Kinetic analysis*. Hydrometallurgy, 66, 37.

DREISINGER D., RICHMOND G., HESS F., LANCASTER T., 2002. *The competitive position of the Mt. Gordon copper process in the copper industry*. ALTA 2002 Copper 7 Forum. ALTA Metalurgical Services, Melbourne, 14.

DREISINGER D.B., STEYL J.D.T., SOLE K.C., GNOINSKI J., DEMPSEY P., 2003. *The Anglo American Corporation/University of British Columbia (AAC/UBC) chalcopyrite process: An integrated pilot–plant evaluation*. in: Rivieros, A., Dixon, D.G., Dreisinger, D.B., Menacho, J. (Eds.), Copper 2003-Cobre 2003, Vol VI, Hydrometallurgy of copper, Montreal, 223–237.

DUTRIZAC J.E., MACDONALD R.J.C., INGRAHAM T.R., 1969, *The kinetics of dissolution of synthetic chalcopyrite in aqueous acidic ferric sulphate solutions*. AIME, 245, 955–959.

FERRON C.J., FLEMING C.A., O'KAN P.T., DREISINGER D.B., 2001, *Application of the PLATSOL process for simultaneous dissolution of copper, nickel, gold, and PGMs from sulfide concentrates and autocatalysts*. Precious Metals, 129–157.

GOK O.S., 2009. *On the role of low-concentration nitrite in oxidative-leaching with oxygen*, PhD Thesis, Colorado School of Mines, CO, USA.

GOK O., ANDERSON C.G., 2013, *Dissolution of Low-Grade Chalcopyrite Concentrate in Acidified Nitrite Electrolyte*, Hydrometallurgy, DOI No: 10.1016/j.hydromet.2013.01.021.

HACKL R.P., DREISIGER D.B., PETERS E., KING J.A., 1995, *Passivation of chalcopyrite during oxidative leaching in sulfate media*. Hydrometallurgy, 39, 25–48.

HIRATO T., KİNOSHITA M., AWAKURA Y., MAJIMA H., 1986, *The leaching of chalcopyrite with ferric chloride*. Metallurgical Transactions B, Process Metallurgy, 17, 19–28.

HIROYOSHI N., MIKI H., HIRAJIMA T., TSUNEKAWA M.A., 2000, *Model for ferrous promoted chalcopyrite leaching*. Hydrometallurgy, 57, 31–38.

JACKSON E., 1982, *Hydrometallurgical extraction and reclamation*. Chichester: Ellis Horwood Ltd., 46-47.

JONES D.L., 1996. *CESL Copper Process*. Alta Copper Hydrometallurgy Forum, Brisbane, Australia, 24.

KAMEOKA Y., PIGFORD R.L., 1977, *Adsorption of nitrogen dioxide into water, sulfuric acid, sodium hydroxide, and alkaline sodium sulfite aqueous solutions*. Ind. Eng. Chem. Fundam., 16, 163–169.

KOFLUK D.K., COLLINS M.J., 1998. *Hydrometallurgical process for the extraction of copper from sulphidicconcentrates*. Chemical Abstract, US Patent No. 5730776.

LEVENSPIEL O., 1972. *Chemical Reaction Engineering*, 2nd ed., John Wiley & Sons, New York, 361–371.

LINGE H.G., 1976. *A study of chalcopyrite dissolution in acidic ferric nitrate by potentiometric titration*. Hydrometallurgy, 2, 51–64.

MARKOVITZ G.Y., SCHWARTZ S.E., NEWMAN L., 1981, *Hydrolysis equilibrium of dinitrogen trioxide in dilute acid solution*. Inorg. Chem., 20, 445–450.

MARSDEN J.O., BREWER R.E., HAZEN N., 2003. *Copper concentrate leaching developments by Phelps Dodge corporation*, Young, C.A. (Ed.), Electrometallurgy and Environmental Hydrometallurgy, TMS, PA, 1429–1446.

MAZET N., 1992, *Modeling of gas–solid reactions*. 1. *Nonporous solids*, Int Chem Eng, 32, 271–284.

MILLER J.D., PORTILLO H.Q., 1979. *Silver catalysis in ferric sulfate leaching of chalcopyrite*. in: Laskowski, J. (Ed.), XIII International Min. Proc. Conf., Elsevier, Amsterdam, 851–901.

MUNOZ P.B., MILLER J.D., WADSWORTH M.E., 1979, *Reaction mechanism for the acid ferric sulfate leaching of chalcopyrite*. Metallurgical Transactions B: Process Metallurgy, 10B, 149–158.

OLANIPEKUN E.O., 1999, *A kinetics study of the leaching of a Nigerian ilmenite ore by hydrochloric acid*. Hydrometallurgy, 53, 1–10.

PAPANGELAKIS V., 2005. *Surface chemistry of molten sulfur on nickel sulfides. Pressure Oxidation-Modelling, Reactor Design, and Processes*. Presentation to CSIRO Minerals Symposium, Perth, Australia, 14th April,

PARK J.Y., LEE Y.N., 1988, *Solubility and decomposition kinetics of nitrous acid in aqueous solution*, J. Phys. Chem., 92, 6294–6302.

STANELY R.W., SUBRAMANIAN K.N., 1977. *Recovering copper from concentrates with insolubale sulfate forming leach*. Chemical Abstract, US Patent No. 4039406.

TSUCHIDA T., NARRITA E., TAKUECHI H., ADACHI M., OKABE T., 1982, *Manufacture of high pure titanium (IV) oxide by the chloride process*. I: *Kinetic study on leaching of ilmenite ore in concentrated hydrochloric acid solution*. Bull. Chem. Soc. Jpn., 55 (6), 1934–1938 (In: Olanipekun, E.O., 1999. Hydrometallurgy 53, 1–10).

VAN WEERT G., FAIR K.J., SCHNEIDER J.C., 1986. *The NITROX process for treating gold bearing arsenopyrite*. In: 116th Annual TMS/AIME Meeting, CO.

WANG S., 2005, *Copper leaching from chalcopyrite concentrates*. J. of Metals, 57, 48–51.

Nomenclature

a order of sodium nitrite concentration

A pre-exponential factor (min^{-1})

b order of particle diameter

b^1 stoichiometric coefficient

C_A bulk concentration of the fluid (mol·m^{-3})

C_{NaNO2} initial concentration of sodium nitrite (M)

D_B effective diffusion coefficient (m^2·s^{-1})

E_A activation energy (kJ·mol^{-1})

k_d apparent reaction rate constant (min^{-1})

k_g rate constant of film diffusion

k_0 constant of semi-emprical equation

k_r rate constant of surface reaction

K equilibrium constant

r_0 radius of unreacted core (mm)

R universal gas constant (J.mol^{-1}·K^{-1})

t reaction time (min)

T temperature (K)

X fractional conversion

ρ_B molar density of B in the solid (mol.m^{-3})

γ_0 initial size of solid particle (mm)